Hierarchical Control of Stand Alone Microgrid for Peak and off-peak Hours Operation

Sourav Chakraborty
Department of Electrical Engineering
National Institute of Technology
Rourkela, India
sourav.er284@gmail.com

Susmita Kar
Department of Electrical Engineering
National Institute of Technology
Rourkela, India
karsusmita@nitrkl.ac.in

Abstract— **Microgrid faces power quality issues like voltage and frequency unbalance due to its low inertia. The limited generation and heterogeneous load switching results in generation scarcity and hence affect the power quality. The intermittent availability of Renewable Energy Sources (RES) also hampers seamless power transfer. Thus, this paper presents a hierarchical control strategy where the primary control strategy maintains the voltage through a closed-loop inverter control technique and frequency through P-f droop mechanism. The secondary control implements a load management strategy to reduce peak demand and maintain frequency through Demand Side Management (DSM) by scheduling Thermostatic Control Loads (TCLs) and grid-tied electric vehicles. In recent scenarios, the usage of such loads is gaining ground hence scheduling results in balancing generation and demand. The voltage and frequency should be maintained adhere to IEEE 1547.1 by taking utmost priority to the customer's comfort. The test system comprises of modified IEEE 13 bus system connected with PV, Battery Energy Storage System (BESS), and Diesel Generator (DZ) for emergency purposes. The hierarchical control strategy is advantageous for peak and off-peak loading conditions with drastic load variation.**

Keywords—Microgrid, Demand Side Management (DSM), Thermostatically Control Loads, Peak Hours, V-f control.

I. INTRODUCTION

The increasing carbon footprint from conventional coal-based power plants motivated us to switch to RES for its easy access and cleanliness. The penetration of RES in the recent era gains potential due to its wide range of availability and lack of carbon emission. The microgrid with RES like solar, and wind face intermittency issues, and hence sophisticated control strategy is required [1]. The low inertia in a microgrid is prone to several abnormalities even with a slight change in load which drives the system to instability, hence a generation side control is required. The ever-increasing demand sometimes leads to the generation shortage; hence, user end control is required. TCL usage, including air conditioners, refrigerators, and geysers, is increasing tremendously. Hence the control of such apparatus makes a lot of difference in power during peak hours. The voltage and frequency deviation are the major concern among them. In [2] the voltage control strategy is implemented through cascaded voltage and frequency controller rather than fails to implement the frequency control. The frequency control strategy is implemented through the virtual inertia concept in dynamic conditions however the voltage control is not implemented as some portions of loads are voltage-dependent and if control operation is not performed it may lead to voltage sag [3]. The inverter control strategy is required along with the auxiliary service due to the intermittency in the availability of RES [4,5]. The voltage and frequency control strategy are implemented in [6] where battery control is also modelled. However, in inverter V-f control directly control the voltage and frequency without clerk and perk transformation, the dynamics in load during peak hours will be high and the system may not able to maintain stability.

The above literature is suitable for off-peak hour control operation when generation ≤ demand. However, during peak hours, user-side control is required for power management [7,8]. The coordination between the voltage control and DSM is established in [9]. However, the frequency control is not presented and the loads comprise only TCLs. The V-f control and DSM are implemented in [10]. Further, dual frequency control is implemented where inverter control and DSM both are responsible for controlling frequency. In [11-13] the peak hour management is done through demand side management. The implementation of DSM for a small change in load make the system more dynamic and also utility service provider will incur additional losses. The ancillary Electric Vehicle Charging Station (EVCS) due to its bidirectional power transfer can also be used to reduce burden during peak hours by taking part in DSM [14]. The grid-tied EV can be fed power to the grid when a certain constraint in voltage and frequency is reached. The generation side control is required during load switching in off-peak hours but in peak hours when demand is more than a generation the end user side control is required [15]. The peak hour can also be classified as an emergency condition when the generation and end-user control are unable to mitigate the demand. The DZ will then provide dynamic inertia to the microgrid and charge the battery [16].

This paper mentioned all the aforementioned gaps and establish better energy management through a hierarchical control strategy.

1. The primary control implemented for voltage control and power sharing. The controller is equipped with pf droop to maintain frequency during off-peak hours.
2. The secondary control strategy incorporate DSM during peak hours for better energy management.
3. The TCLs and EVCS act as virtual battery storage that is implemented during peak hours to mitigate generation and demand mismatch.
4. The coordination among the micro sources and DSM is established to mitigate abnormalities by validating in the modified IEEE 13 bus system.

978-1-6654-5930-3/22/$31.00 ©2022 IEEE

II. System Under Consideration

The system taken under consideration comprise of modified IEEE 13 bus system having connected with PV and BESS as sources and also comprises three phases of TCLs (24%) loads distributed among the buses. The single-line diagram is shown in Fig.1. The series stings and parallel stacks of PV taken as 105 and 37 respectively, and BESS having 200V of 5 series strings and 102 parallel stacks having a rated capacity of 6.68Ah are taken into consideration where the line parameters are obtained from [17].

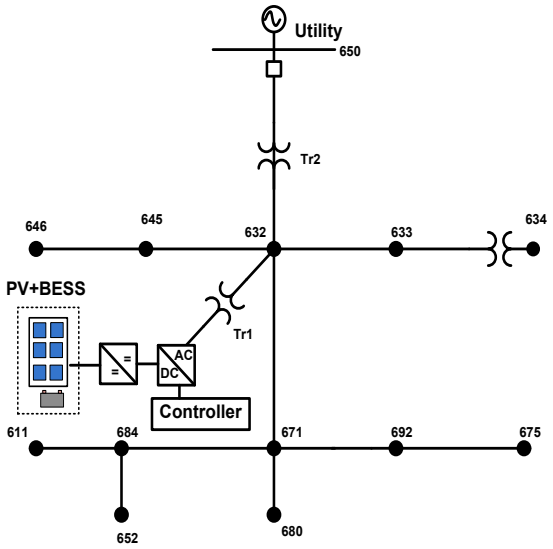

Fig 1. Modified IEEE 13 bus system

III. Primary Voltage and Frequency Control

The primary voltage control is established through the PV inverter control strategy and frequency control is established through the pf droop technique. In order to ensure a smooth transfer of power in the stand-alone mode of operation, the P-f droop-based cascaded voltage and current control in the d-q reference frame have been devised as shown in Fig 2. In this technique voltage and current are depicted in the space-vector form which is a general way of representing spatially distributed electrical quantities, having magnitude (A) and phase (ϕ) in a three-phase system. The d-q axis rotates synchronously with the space vector such that the relative velocity between them becomes zero thereby generating a DC signal from a three-phase system. In this space vector-based droop control strategy, the modelling has been done referring [18] where the voltage controller controls the output voltage and provides reference to the current controller that controls the current. In this case, the frequency is being measured also and controlled from the P-f droop. The three-phase voltage and currents are sensed from PCC (632) and feedback is taken; hence the three-phase power is measured.

The three-phase voltage is transformed into the direct and quadrature form. The *P-f* droop coefficient is given as:

$$m_{\mathrm{p}} = (\omega_{\max} - \omega_{\min})/P_{\max} \tag{1}$$

For a more straightforward manner of system representation, the d-q voltages and currents, expressed in the form of vectors, are given in (2).

$$\Delta V_{\mathrm{o}}^{*} = \begin{bmatrix} V_{\mathrm{d\text{-}0}}^{*} \\ V_{\mathrm{q\text{-}0}}^{*} \end{bmatrix} = \begin{bmatrix} V_{dc} \\ 0 \end{bmatrix};\ \Delta V_{\mathrm{o}} = \begin{bmatrix} V_{\mathrm{d\text{-}0}} \\ V_{\mathrm{q\text{-}0}} \end{bmatrix};\ \Delta I_{\mathrm{in}} = \begin{bmatrix} I_{\mathrm{d\text{-}in}} \\ I_{\mathrm{q\text{-}in}} \end{bmatrix};\ \Delta I_{\mathrm{o}} = \begin{bmatrix} I_{\mathrm{d\text{-}0}} \\ I_{\mathrm{q\text{-}0}} \end{bmatrix} \tag{2}$$

Where, ΔV_o^* is voltage control's reference values. $\Delta \mathrm{V}_o$ is the inverter's output voltage (at the filter capacitor) measured in the d-q frame, $\Delta \mathrm{I}_{in}$ displays the d-q current components obtained from the inverter measured before the LCL filter and ΔI_o depicts the output currents in the d-q frame obtained after the LCL filter. The outputs of the voltage control block serve as the reference values for the current control block and are given as:

$$I_{\mathrm{d\text{-}in}}^{*} = \left[\left\{ \left(V_{\mathrm{d\text{-}o}}^{*} - V_{\mathrm{d\text{-}o}} \right) \left(K_{\mathrm{p\text{-}v}} + \int K_{\mathrm{i\text{-}v}} dt \right) \right\} + I_{\mathrm{d\text{-}o}} - \frac{V_{\mathrm{q\text{-}o}}}{X_{\mathrm{Cf}}} \right] \tag{3}$$

$$I_{\mathrm{q\text{-}in}}^{*} = \left[\left\{ \left(V_{\mathrm{q\text{-}o}}^{*} - V_{\mathrm{q\text{-}o}} \right) \left(K_{\mathrm{p\text{-}v}} + \int K_{\mathrm{i\text{-}v}} dt \right) \right\} + I_{\mathrm{q\text{-}o}} - \frac{V_{\mathrm{d\text{-}o}}}{X_{\mathrm{Cf}}} \right] \tag{4}$$

The direct and quadrature reference signals λ_d and $\lambda_q$respectively, which are obtained as the end result of the current control block are given as:

$$\lambda_{\mathrm{d}} = \left[\left(I_d^{*} - I_{\mathrm{d\text{-}in}} \right) \left(K_{\mathrm{p\text{-}i}} + \int K_{\mathrm{i\text{-}i}} dt \right) \right] - I_{\mathrm{q\text{-}in}} X_{\mathrm{L}f} \tag{5}$$

$$\lambda_q = \left[\left(I_q^{*} - I_{\mathrm{q\text{-}in}} \right) \left(K_{\mathrm{p\text{-}i}} + \int K_{\mathrm{i\text{-}i}} dt \right) \right] - I_{\mathrm{d\text{-}in}} X_{\mathrm{L}f} \tag{6}$$

Where, X_{L_f} and X_{C_f} are the inductive and capacitive reactance of the LCL filter, respectively. The current loop PI gains are $K_{p-i} = 29.86$ and $K_{i-i} = 200.153$ respectively, while the voltage controller PI gains are $K_{p-v} = 0.1$ and $K_{i-v} = 100.24$ respectively which has been calculated using Ziegler–Nichol's method. The droop values are presented in Table I.

The frequency control is done through pf droop-based Battery Energy Storage System (BESS), where the under-frequency is rectified through battery discharging and over-frequency can be rectified through battery charging. Monitoring the battery's state of charge (SOC) is essential as the level of discharging has a significant effect on the battery's life-cycle [19]. The SoC can be determined using Eq.7

$$\mathrm{SOC} = \left[1 - \frac{\int_0^t i_{batt} dt}{Q_{charge}} \right] \times 100\% \tag{7}$$

When the P.V and BESS system is unable to meet the critical demand, a diesel generator (DZ) is present as a backup power supply.

TABLE I. Droop Values

$m_{p(PV)}$	$m_{p(BESS)}$
0.0000375	0.0000372

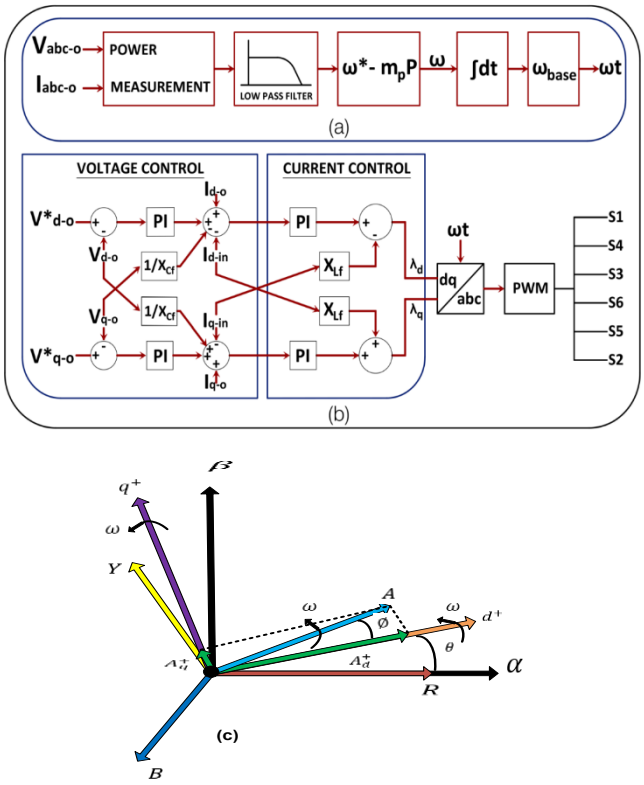

Fig. 2 (a) pf Droop (b) Voltage Control Strategy (c) Vector Representation

IV. Demand Side Management (Secondary Control)

The DSM is implemented during peak hours as a secondary control unit through the manipulation of TCLs [20]and EVCS [21]. The TCLs in the recent era is gaining ground almost in every sector and hence manipulation of such loads makes a big difference in supply and demand. The heterogeneous distribution of TCLs in resident sector makes it difficult to aggregate and hence the aggregate flexibility of TCLs with N>>1 is given as

$$\frac{dS(t)}{dt} = -\frac{1}{\hat{\tau}}\,\mathrm{S(t)} + \mathrm{P(t)} \tag{8}$$

Eq. 8 depicts the aggregation of TCLs as a single energy storage model having an evaporative term with total energy of (S(t)) and power (P(t)). $\hat{\tau}$ (h) is the time constant for the population model. The temperature verifier with check the θ_{min} and θ_{max} of the operating TCLs. The temperature transition of TCLs given in Eq. 9

$$C_i^t = C_i^{t-1} + ins_i(C_S^t - C_i^{t-1}) + con_j y_i^{t-1} \tag{9}$$

Where,

C_i^t= TCLs temperature

C_S^t= Surrounding temperature

ins_i =Parameter related to decay of temperature due to insulation

con_j= Electrical to thermal conversion factor.

The TCLs constraints are given in equation 10, 11

$$y_i^{min} \le y_i^t \le y_i^{max} \tag{10}$$

$$y_i^t = 0, t < OT_i, t > FT_i \tag{11}$$

Where, OT_i and FT_i are the time when the operating TCLs will turn on and off respectively.

The final stage is to take the decision and give signal to individual TCLs. The Decision unit having TCLs constraint and the final signal sent through low bandwidth communication network. The flow chart shown in Fig. 3 Where it is observed that underfrequency is managed by inverter controller and DSM. Further when the frequency fall below 50Hz the inverter controller action will take place but during peak hours when frequency fall below 47Hz the DSM will be implemented and hence generation will equalize the demand thus proving it as a virtual energy storage system.

The grid-tied electric vehicle also played a major role during peak hours and provide additional support by supporting during scarcity. During the off-peak hours, the excess power is fed to the EV while it discharge itself when required. The EV charging station is basically equipped with a battery storage and a bidirectional converter with limiter. The usage of limiter is to limit the discharge of battery when feeding to the grid i.e up to 55% SOC. The rest of the charge is reserved for the EV charging.

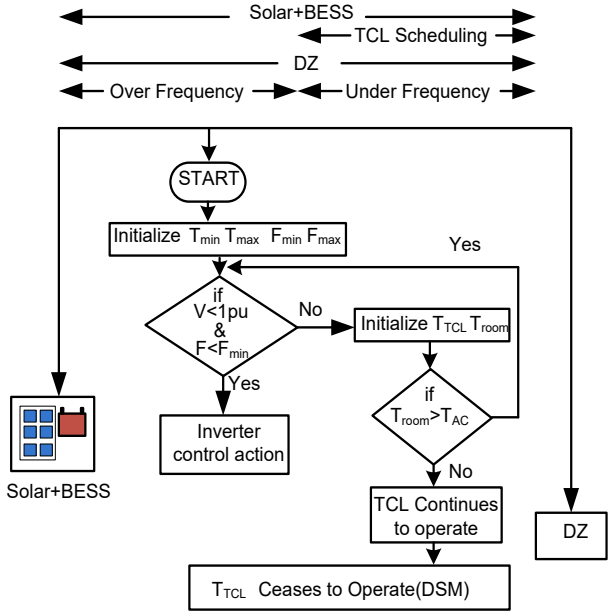

Fig.3 Flow chart showing voltage and frequency control during abnormalities

The operation of TCLs is depicted in below equation

$$\beta = \begin{Bmatrix} 1 & Q_{Min} < Q < Q_{Max} \\ 0 & Q < Q_{Min} \\ Charging & Otherwise \end{Bmatrix} \tag{12}$$

Where,

β = Boolean Variable that takes decision on power flow to the grid.

Q_{Min} = Minimum Charge (55%).

Q_{Max} = Maximum Charge (100%)

The coordination of primary and secondary control strategy makes the system stable and reduce the gap between generation and demand. The subsequent section shows the results of the above methodology.

V. Results and Discussions

The results of the hierarchical operation of control strategy is presented. The solution and validation of abnormalities during peak and off-peak hours is shown in subsequent subsections.

A. Off-Peak Hours

The voltage during steady state operation is shown in Fig. 4.

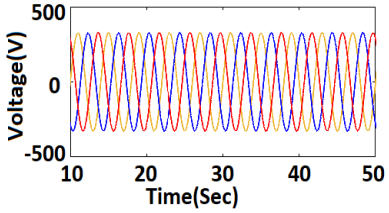

Fig. 4 Three Phase Voltage During Steady State

The 28% load is suddenly added in bus 646 the voltage controller tries to maintain the voltage to 1pu as shown in Fig. 5. The corresponding frequency response is shown in Fig. 6 where it is observed that battery unit and PV responsible for sharing the load and is the battery SOC is shown in Fig. 7.

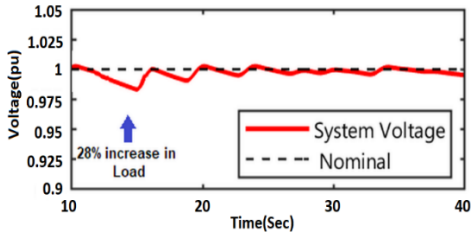

Fig. 5 RMS Voltage at Bus 632 when Load increased to 28%

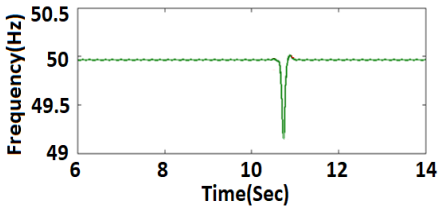

Fig. 6 Frequency at Bus 632 when Load increases to 28%

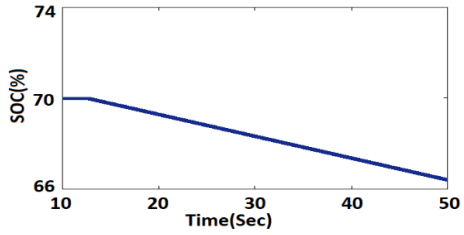

Fig. 7 Battery State of Charge

The scenario arises when 15% of the load is removed suddenly from Bus 632. The over frequency arises as shown in Fig. 8.

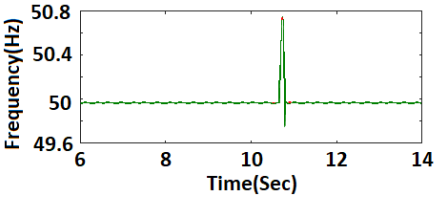

Fig 8 Frequency at Bus 632 when Load decreases to 15%

The case can be irradicate through battery charging. Fig. 9 shows the battery SOC during charging state.

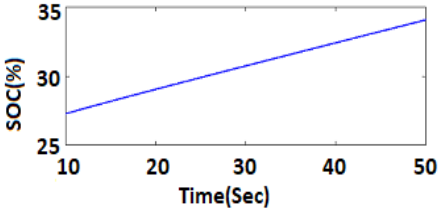

Fig. 9 Battery State of Charge

B. Peak Hours

The Peak hours arises when the generation is less compared to demand. In this case the generation and demand mismatch can be mitigated through load management technique. The TCLs are manipulated in this scenario based on the frequency of the system. In this case a total 500 number of TCLs are taken into consideration. During under frequency the TCLs are manipulated based on temperature band as shown in Fig 10 and Fig. 11 respectively. The Voltage is maintained at 1pu as shown in Fig. 12

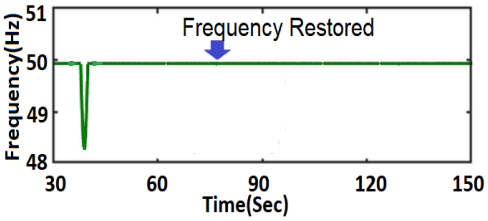

Fig. 10 Frequency at Bus 632 when Load increases by 35%

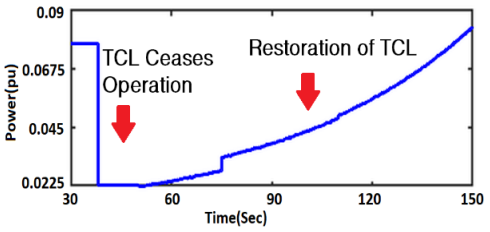

Fig 11. TCLs Power during Under Frequency

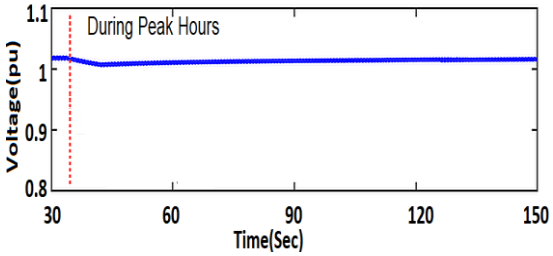

Fig. 12 Voltage measured at Bus 671 During Load Change

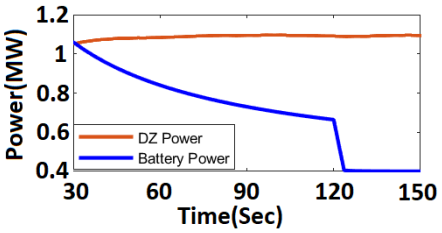

Fig. 13 Diesel Generator Power

The case arises during peak hours when the PV, BESS and load management unable to mitigate the load demand. The DZ will came into action and deliver the loads and charge the battery as shown in Fig 13

VI. Conclusion

The hierarchical control strategy implemented is able to maintain stability and power quality in stand-alone microgrid during off-peak and peak hour. The primary voltage controller and droop-based frequency controller maintaining the voltage and frequency respectively during off-peak hours whereas the secondary control operated through DSM maintain frequency by manipulating TCLs in peak hours. The temperature band of (16-22)°C is taken into consideration for TCLs manipulation. The load management is implemented based on the frequency of operation without hampering the Customer's thermal comfort. The voltage and frequency is maintained adhere to IEE1547.1 both during peak and off peak hours.

References

[1] T. Wu, G. Bao, Y. Chen, and J. Shang, "A Review for Control Strategies in Microgrid," in 2018 37th Chinese Control Conference (CCC), Jul. 2018, vol. 73, no. 2, pp. 30–35.

[2] F. Doost Mohammadi, H. Keshtkar, A. Dehghan Banadaki, and A. Feliachi, "A novel cooperative distributed secondary controller for VSI and PQ inverters of AC microgrids," Heliyon, vol. 5, no. 6, p. e01823, 2019.

[3] A. Fathi, Q. Shafiee, and H. Bevrani, "Robust frequency control of microgrids using an extended virtual synchronous generator," IEEE Transactions on Power Systems, vol. 33, no. 6, pp. 6289–6297, 2018

[4] J. Hu, Y. Xu, K. W. Cheng, and J. M. Guerrero, "A model predictive control strategy of PV-Battery microgrid under variable power generations and load conditions," Applied Energy, vol. 221, no. December 2017, pp. 195–203, 2018.

[5] M. J. Sanjari and H. Karami, "Optimal control strategy of battery-integrated energy system considering load demand uncertainty," Energy, vol. 210, p. 118525, 2020.

[6] S. Adhikari and F. Li, "Coordinated V-f and P-Q control of solar photovoltaic generators with MPPT and battery storage in microgrids," IEEE Transactions on Smart Grid, vol. 5, no. 3, pp. 1270–1281, 2014.

[7] S. Chakraborty, S. Kar, and D. Kumar, "Review of Demand Side Management with Thermostatically Controllable Loads," 2021 IEEE 2nd International Conference on Electrical Power and Energy Systems, ICEPES 2021, pp. 1–5, 2021.

[8] D. Groppi, A. Pfeifer, D. A. Garcia, G. Krajačić, and N. Duić, "A review on energy storage and demand side management solutions in smart energy islands," Renewable and Sustainable Energy Reviews, vol. 135, no. April 2020, 2021.

[9] S. Bera, S. Chakraborty, D. Kumar, N. Ali, and M. Lehtonen, "Optimal deep learning based aggregation of TCLs in an inverter fed stand-alone microgrid for voltage unbalance mitigation," Electric Power Systems Research, vol. 210, no. June, p. 108178, 2022.

[10] S. Chakraborty, P. Arvind, and D. Kumar, "Coordinated Control for Frequency Regulation in a Stand-Alone Microgrid Bolstering Demand Side Management Capability," Electric Power Components and Systems, vol. 49, no. 1–2, pp. 1–17, 2021.

[11] I. Jendoubi, K. Sheshyekani, and H. Dagdougui, "Aggregation and Optimal Management of TCLs for Frequency and Voltage Control of a Microgrid," IEEE Transactions on Power Delivery, vol. 36, no. 4, pp. 2085–2096, 2021.

[12] S. Noor, W. Yang, M. Guo, K. H. van Dam, and X. Wang, "Energy Demand Side Management within micro-grid networks enhanced by blockchain," Applied Energy, vol. 228, no. July, pp. 1385–1398, 2018.

[13] Elisa Guelpa, Ludovica Marincioni, Stefania Deputato, Martina Capone, Stefano Amelio, Enrico Pochettino, and Vittorio Verda. Demand side management in district heating networks: A real application. Energy, 182:433–442, 2019.

[14] S. Faddel, S. Member, and O. A. Mohammed, "Automated distributed electric vehicle controller for Residential Demand Side Management," IEEE Transactions on Industry Applications, vol. 55, no. 1, pp. 16–25, 2019.

[15] Ngoc An Luu. Control and management strategies for a microgrid. PhD thesis, Universit´e de Grenoble, 2014.

[16] J. Xiao, L. Bai, F. Li, H. Liang, and C. Wang, "Sizing of energy storage and diesel generators in an isolated microgrid Using Discrete Fourier Transform (DFT)," IEEE Transactions on Sustainable Energy, vol. 5, no. 3, pp. 907–916, 2014.

[17] W. H. Kersting, "Radial distribution test feeders," Proceedings of the IEEE Power Engineering Society Transmission and Distribution Conference, vol. 2, no. WINTER MEETING, pp. 908–912, 2001.

[18] Z. Liu, J. Liu, and Y. Zhao, "A unified control strategy for three-phase inverter in distributed generation," IEEE Transactions on Power Electronics, vol. 29, no. 3, pp. 1176–1191, 2014.

[19] J. Asakura and H. Akagi, "State-of-Charge (SOC)-Balancing Control of a Battery Energy Storage System Based on a Cascade PWM Converter," IEEE Transactions on Power Electronics, vol. 24, no. 6, pp. 1628–1636, 2009.

[20] Y. Ding, D. Xie, H. Hui, Y. Xu and P. Siano, "Game-Theoretic Demand Side Management of Thermostatically Controlled Loads for Smoothing Tie-Line Power of Microgrids," in *IEEE Transactions on Power Systems*, vol. 36, no. 5, pp. 4089-4101, Sept. 2021.

[21] M. H. K. Tushar, A. W. Zeineddine, and C. Assi, "Demand-Side Management by Regulating Charging and Discharging of the EV, ESS, and Utilizing Renewable Energy," IEEE Transactions on Industrial Informatics, vol. 14, no. 1, pp. 117–126, 2018.